Applied Clay Science 49 (2010) 324–329

Contents lists available at ScienceDirect

Applied Clay Science

journal homepage: www.elsevier.com/locate/clay

Antioxidant drugs intercalated into layered double hydroxide: Structure and *in vitro* release

Xianggui Kong, Lan Jin, Min Wei *, Xue Duan

State Key Laboratory of Chemical Resource Engineering, Beijing University of Chemical Technology, Beijing 100029, China

ARTICLE INFO

Article history:
Received 4 December 2009
Received in revised form 15 June 2010
Accepted 16 June 2010
Available online 23 June 2010

Keywords:
Layered double hydroxide
Composites
Pharmaceuticals
Kinetics
Mass transfer
Antioxidant drugs

ABSTRACT

Two representative antioxidant drugs, carnosine and gallic acid (denoted as GA), were intercalated into Mg/Al layered double hydroxide (LDH) by ion exchange and coprecipitation. A gradual and biphasic *in vitro* release behavior of the drugs from LDH in pH = 7.4 phosphate buffered saline (PBS) was observed, and no burst release phenomenon was noticed at the beginning of release tests. Furthermore, two kinetics models (modified Freundlich model and parabolic diffusion model) were chosen to simulate the release kinetics of the drugs from LDH. The release process involved two stages: firstly surface diffusion and secondly intraparticle diffusion. In addition, the effect of the drug-LDH on scavenging 2, 2-diphenyl-1-picrylhydrazyl (DPPH) radicals was studied. Both carnosine and GA released from the LDH matrix served as excellent antioxidants to scavenge DPPH radicals in a long release period (scavenging ratio: 95.9% for carnosine-LDH and 83.9% for GA-LDH in 870 min). Therefore, this work provides a facile approach for the encapsulation of unstable antioxidant drugs in LDH materials and for controlled drug release.

© 2010 Elsevier B.V. All rights reserved.

1. Introduction

Searching for efficient and safe transport vehicles to delivery drugs and bioactive molecules into cells was a challenging and exciting area of research since the direct delivery of these beneficial agents is generally inefficient and suffers from problems such as destroyed by stomach acid, metabolized by pancreatic enzymes and other considerable side effect (Azzam and Domb, 2004; Dietz and Bahr, 2004; Feng and Chien, 2003; Minko, 2004). Taking into account these aspects, many materials were studied for their drug delivery capabilities. Polymers, over the past decade, were widely studied as delivery carriers (Theodorou, 2007; Kelner and Schacht, 2005). However, the degradation of synthetic polymers caused unwanted toxic effects (Couvreur et al., 1995). Inorganic materials (*e.g.* calcium phosphate, carbon materials, silicon oxides and iron hydroxides) are becoming strong competitors owing to many advantages, including wide availability, good hydrophilicity and biocompatibility, promising capability of targeted delivery and controlled release of carried drugs. Therefore, much attention has been devoted to various inorganic materials as novel non-viral and cellular delivery vectors (Gomes and Silva, 2007; Barbe et al., 2004; Bauer et al., 2004; Tammaro et al., 2009).

Layered double hydroxides (LDHs), with general formulation of $[M^{2+}_{1-x}M^{3+}_{x}(OH)_2]^{x+}(A^{n-})_{x/n}\cdot mH_2O$, were extensively applied in the fields of catalysis (Wei et al., 2007; Yu et al., 2009), molecular recognition (Fogg et al., 1998; Fogg et al., 1999), functional materials (Leroux et al., 2005; Leroux et al., 2009) and drug carrier (Khan et al., 2001; Hoyo, 2007; Costantino et al., 2008;). LDH materials, especially MgAl/LDH, possess the advantages of low-cost preparation, biocompatibility and less toxicity to mammalian cells (Shi et al., 2007; Kriven et al., 2004; Kwak et al., 2004). MgAl/LDH can be quickly absorbed by various cell lines based on the conjugation of specific antibody and biodegraded in the cytoplasm (Choy et al., 2001; Tyner et al., 2004; Xu et al., 2006). Consequently, a series of pharmaceutically active compounds like ibuprofen, fenbufen, diclofenac, camptothecin, prednisone, vitamin, eusolex, etc., were intercalated into LDHs and demonstrated the feasibility of LDH-based drug delivery systems (Williams and O'Hare, 2006; Joshi et al., 2009; Ambrogi et al., 2001; Dagnon et al., 2009).

Free radicals, including the 2, 2-diphenyl-1-picrylhydrazyl (DPPH) radical, hypochlorite radicals and hydroxyl radical not only cause damage to nucleic acids, proteins, and membrane lipids but also contribute to the aging process of the cells and act as a trigger to various diseases (Kitts and Weiler, 2003). Carnosine (β-alanyl-L-histidine, Fig. 1A) and gallic acid (3,4,5-trihydroxybenzoic acid, denoted as GA, Fig. 1B), well known for their antioxidant properties (Friedman and Jürgens, 2000; Decker et al., 2000), can terminate the attacks of free radicals and reduce the risk of diseases. Furthermore, carnosine and GA exhibit other biological activities in human health such as antivirus, antiallergic, antiglycation and α,β-unsaturated carbonyl scavenger (Vaughan-Jones et al., 2006; Galati and O'Brien, 2004). However, both carnosine and GA are easily oxidized under

* Corresponding author. Tel.: +86 10 64412131; fax: +86 10 64425385.
E-mail address: weimin@mail.buct.edu.cn (M. Wei).

0169-1317/$ – see front matter © 2010 Elsevier B.V. All rights reserved.
doi:10.1016/j.clay.2010.06.017

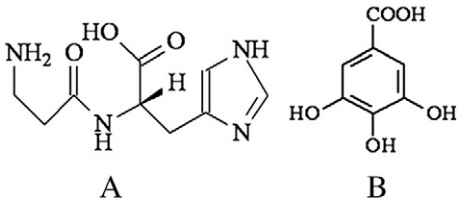

Fig. 1. Structure of (A) carnosine and (B) gallic acid.

mild conditions and show sensitivity to pH, which decreases their biofunctionality. In addition, rapid hydrolysis in blood for carnosine and short plasma half-life for GA also limit their manipulation. As a result, searching drug delivery and controlled release system for carnosine and GA is an effective solution for overcoming such problems.

Our previous work demonstrated that both chemical and stereochemical stability of chiral drug L-dopa were enhanced significantly after intercalation into LDH (Wei et al., 2008). In the present study, carnosine and GA, selected as models for antioxidant drugs, were intercalated into MgAl/LDH by ion exchange and coprecipitation. Controlled release behavior of the two drugs from LDH matrix was studied in pH = 7.4 buffer solution. The ability of the drug-LDH for scavenging free radicals was also investigated.

2. Experimental section

2.1. Reagents

Carnosine, GA and DPPH were purchased from Aldrich; Mg $(NO_3)_2 \cdot 6H_2O$, $Al(NO_3)_3 \cdot 9H_2O$, Na_2CO_3 and NaOH were purchased from Beijing Chemical Co. Limited. All chemicals were of analytical grade and used without further purification. Phosphate buffered saline was used at 37 °C.

2.2. Preparation and characterization

2.2.1. Synthesis of drug-LDH

NO_3-LDH was synthesized by hydrothermal reaction (Bontchev et al., 2003). Carnosine-LDH was prepared via ion exchange. The NO_3-LDH (8.3 g, freshly prepared pasty sample, ca. 2 mmol of dried sample) was dispersed in a solution of carnosine (0.95 g, ca. 4 mmol) in deionized water with vigorous agitation under nitrogen atmosphere. The dispersion (pH about 9.5) was kept for 48 h at 70 °C. The precipitate was washed thoroughly, centrifuged and dried in a vacuum desiccator at room temperature for 48 h.

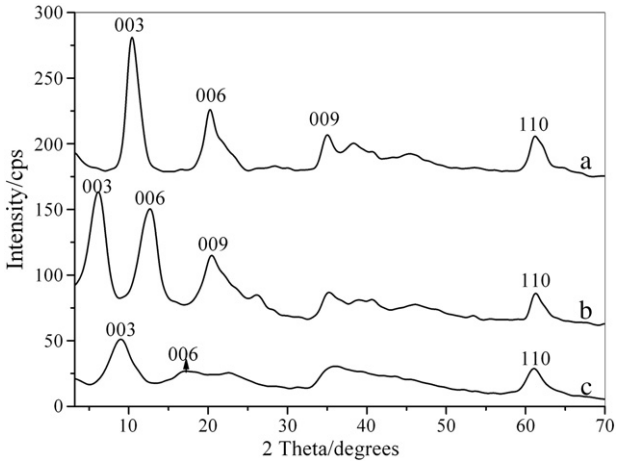

Fig. 2. XRD patterns of (a) NO_3-LDH, (b) carnosine-LDH and (c) GA-LDH.

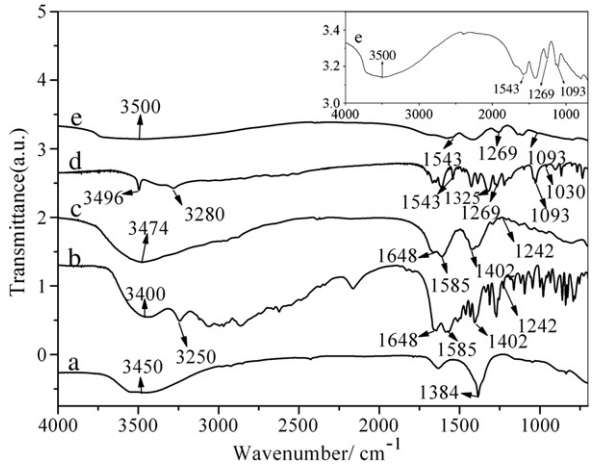

Fig. 3. FI-IR spectra of (a) NO_3-LDH, (b) pristine carnosine, (c) carnosine-LDH, (d) pristine GA and (e) GA-LDH. The inset is the enlarged view of (e).

GA-LDH was synthesized by coprecipitation. An aqueous solution (100 ml, 1.0 M) of NaOH and a mixed solution (50 ml) of 0.2 M Mg $(NO_3)_2 \cdot 6H_2O$ and 0.1 M $Al(NO_3)_3 \cdot 9H_2O$ were simultaneously added dropwise into a GA solution (50 ml, 0.02 mol) under a nitrogen atmosphere with vigorous stirring until the final pH of ca. 8 was obtained. The resulting dispersion was aged avoiding sunlight at 40 °C for 24 h. The product was filtered, washed thoroughly with water and finally dried in vacuum at room temperature for 48 h.

2.2.2. In vitro drug release

A known amount of LDH (3.0 g of carnosine-LDH and 0.1 g of GA-LDH) was dispersed in 300 ml phosphate buffered solution (PBS) solution with pH = 7.4, followed by incubation in a water bath at 37 °C with gentle shaking. A certain volume of solution (1.0 ml and 2.0 ml for carnosine-LDH and GA-LDH, respectively) was withdrawn, separated through a 0.2 μm syringe filter at predetermined time periods and added into equal volumes of fresh PBS. The amount of released carnosine was measured by using the reaction with DPPH (Terashima et al., 2007). Equal-volume solutions of carnosine and DPPH (0.2 mg/ml in ethanol) were mixed and placed in the dark for 20 min at room temperature. The absorbance at 517 nm was measured with a UV–vis spectrophotometer. The amount of released GA was measured at 259 nm. Runs were performed in triplicate. To

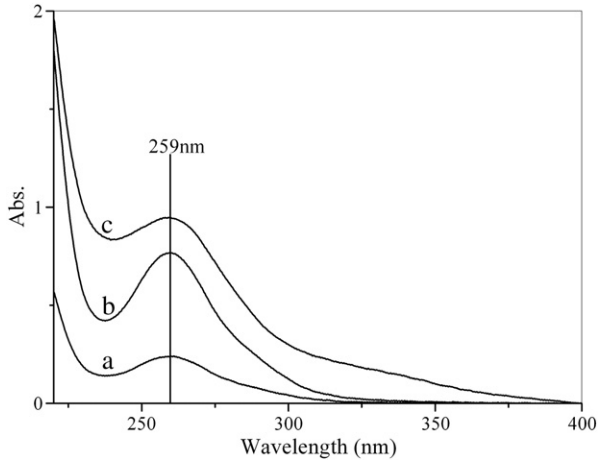

Fig. 4. UV–vis spectra of (a) GA released from GA-LDH after 15 min, (b) pristine GA (0.015 mg/ml) and (c) GA released from GA-LDH after 120 min.

determine the amount of drug corresponding to total release, Na_2CO_3 (0.5 g) was dissolved in dispersion with the above composition and stirred for 2 h. The drug concentration was determined as described. After the release test, carnosine-LDH and GA-LDH residues were collected and dried at 70 °C for 48 h. The residues were named as carnosine-LDH-R and GA-LDH-R.

2.2.3. Measurements of radical scavenging

A test sample (0.02 g of carnosine-LDH and GA-LDH) was dispersed in a quartz cell with 2 ml of PBS (pH = 7.4) and 2 ml of DPPH solution (0.2 mg/ml in ethanol). The absorbance at 517 nm was measured with a UV–vis spectrophotometer at predetermined times.

$$\text{scavenging ratio} = [1-(\text{Abs})_t / (\text{Abs})_0] \times 100\%$$

$(\text{Abs})_t$ and $(\text{Abs})_0$ are the absorbance of the solution at the time 0 and t.

2.2.4. Characterization

Powder X-ray diffraction patterns were recorded by the Shimadzu XRD-6000 power X-ray diffractometer using Cu Kα radiation ($\lambda = 0.154$ nm) at 40 kV, 30 mA, a scanning rate of 10° min^{-1}, and a 2θ angle ranging from 3° to 70°. UV–vis absorption spectra were performed on the Shimadzu UV-2501PC spectrometer. Fourier transform infrared (FT-IR) spectra were recorded using the Vector 22 (Bruker) spectrophotometer using the KBr pellet technique in the range 4000–400 cm^{-1} with 2 cm^{-1} resolution. Microanalysis was performed by inductively coupled plasma (ICP) emission spectroscopy on the Shimadzu ICPS-7500 instrument using solutions prepared by dissolving the samples in dilute HCl. Carbon, hydrogen and nitrogen analyses were carried out with the Elementarvario elemental analysis instrument.

3. Results and discussion

3.1. Characterization of drug-LDH

The powder X-ray diffraction patterns of the drug-LDH hybrids were shown in Fig. 2. The basal spacing d_{003}, representing the thickness of the brucite layer plus the interlayer space, is a function of the size and orientation of the intercalated anions. Compared with the NO_3-LDH (Fig. 2a, $2\theta = 10.38°$, $d_{003} = 0.88$ nm), the expansion of the basal spacing of carnosine-LDH (Fig. 2b, $2\theta = 5.83°$, $d_{003} = 1.51$ nm) and GA-LDH (Fig. 2c, $2\theta = 8.71°$, $d_{003} = 1.01$ nm) indicated the intercalation of carnosine and GA. The (110) reflection ($2\theta = 61°$) showed no obvious shift compared with NO_3-LDH, indicating that no significant change occurred in the LDH host layers after incorporation of the drugs.

The FT-IR spectra were shown in Fig. 3. For the sake of clarity, only the main absorption bands were listed. The spectrum of NO_3-LDH (Fig. 3a) showed a broad absorption band at 3450 cm^{-1} due to the stretching vibration of the hydroxyl groups of the LDH layers and interlayer water molecules. The band at 1384 cm^{-1} belongs to the stretching vibration of NO_3^-. In the spectrum of carnosine (Fig. 3b), the bands centered at 3400 and 3250 cm^{-1} belong to ν(O—H) and ν(N—H) vibrations, and those at 1648, 1585, 1402 and 1242 cm^{-1} were attributed to ν(C=O), ν_{as}(COO), ν_s(COO) and ν(C—N), respectively. In the case of carnosine-LDH (Fig. 3c), the broad absorption band at about 3474 cm^{-1} was assigned to O—H group stretching and deformation vibration of the hydroxide groups and interlayer water molecules. Characteristic absorption bands of carnosine were observed at 1648, 1585, 1402 and 1242 cm^{-1}. The spectrum of GA (Fig. 3d) displayed bands at 3496 and 3280 cm^{-1} corresponding to free phenolic O–H stretching and carboxyl O–H stretching vibrations. Bands at 1543 and 1325 cm^{-1} belong to C=C stretching and in-plane O–H bending vibration, and those at 1093 and 1030 cm^{-1} are due to aromatic C–H deformation. After intercalation, the characteristic bands of GA were observed at 1543, 1269 and 1093 cm^{-1} in the case of GA-LDH (Fig. 3e).

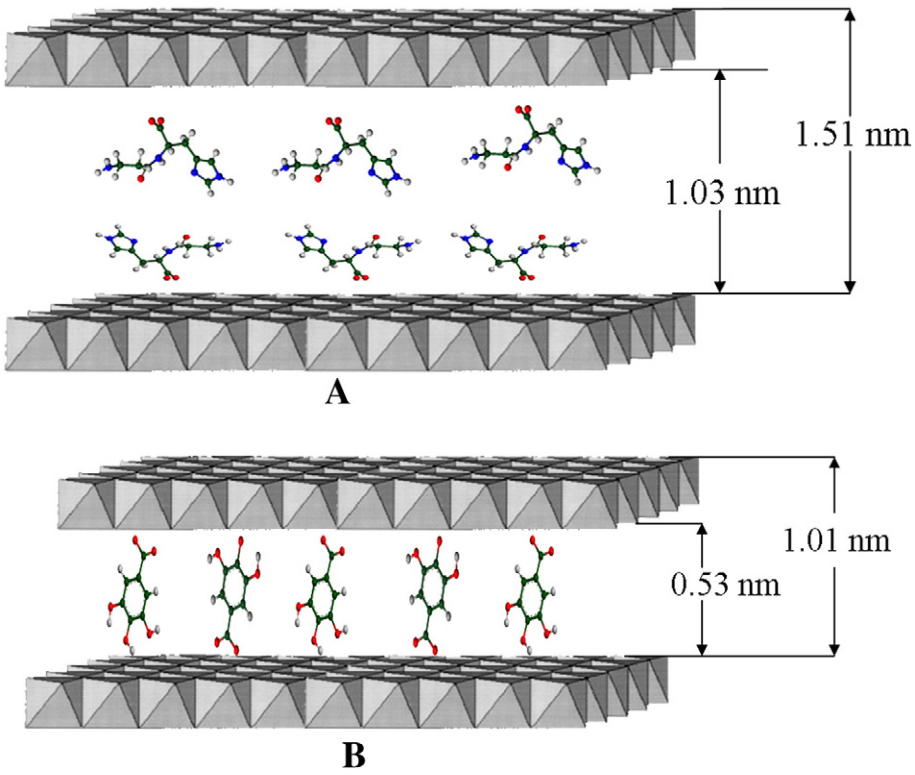

Scheme 1. Proposed structure of (A) carnosine-LDH and (B) GA-LDH.

A broad absorption band at ~ 3500 cm^{-1} is attributed to the O–H stretching of hydroxyl groups in LDH and the phenolic OH groups.

Fig. 4 displays the UV–vis spectra of GA released from GA-LDH after 15 and 120 min. The absorption band at 259 nm for the released GA was found at the same wavelength as pristine GA. The intensity increased from 15 to 120 min release. Oxidation of GA to quinone was restrained to some extent, since no obvious absorption bands at ~320 and 380 nm were observed after 120 min, in contrast to the previous report of the oxidation of GA in water during 15 min (José and Cristina, 2010).

3.2. Structural models and chemical compositions for carnosine-LDH and GA-LDH

According to the elemental analysis (Mg 10.15%, Al 5.37%, C 17.29%, N 9.59%, H 4.80% for carnosine-LDH; Mg 12.41%, Al 6.58%, C 14.25%, N 0.12%, and H 4.07% for GA-LDH), the chemical formula can be expressed as $Mg_{0.68}Al_{0.32}(OH)_2(C_9H_{13}N_4O_3)_{0.24}(C_9H_{12}N_4O_3)_{0.01}(NO_3)_{0.06}\cdot 2.0H_2O$ for carnosine-LDH and $Mg_{0.68}Al_{0.32}(OH)_2(C_7H_5O_5)_{0.13}(C_7H_4O_5)_{0.09}(NO_3)_{0.01}\cdot 1.8H_2O$ for GA-LDH. Both the N/C ratios (0.56 and 0.008 for carnosine-LDH and GA-LDH, respectively) were larger than that of the drugs (carnosine: 0.53; GA: 0), indicating little amounts of NO_3^- coexisting in the interlayer space. The content of intercalated carnosine and GA accounts for 80.6% and 95.6% (molar percentage) of the total guest anions. Taking into account the interlayer spacing of 1.51 and 1.01 nm for carnosine-LDH and GA-LDH, the interlayer thickness is 1.03 nm (carnosine-LDH) and 0.53 nm (GA-LDH), by subtracting the thickness of 0.48 nm for the LDH layer (Prevot et al., 1998). Carnosine and GA dissociate in three steps and four steps respectively in aqueous solution. Carnosine: $pKa_1 = 2.7$, $pKa_2 = 7.1$ and $pKa_3 = 10.6$ (Friedrich et al., 1986); GA: $pKa_1 = 4.3$, $pKa_2 = 8.8$, $pKa_3 = 11.4$ and $pKa_4 = 11.7$ (Giannakopoulos et al., 2005). According to the synthesis pH value (9.5 and 8.0 for carnosine and GA), the distribution coefficients of the monovalent and bivalent anion were calculated to be 92.3% and 7.3% for carnosine and 86.3% and 13.6% for GA, indicating the overwhelming majority of the monovalent anion in the synthesis process. This is in accordance with the chemical formulae of the two drug-LDH composites, in which both monovalent and bivalent anions were intercalated. Taking into account the length of the carnosine and GA anion (1.21 nm for carnosine and 0.65 nm for GA, calculated from the formula optimized by the density functional theory (DFT) at B31YP/6–31G (d,p) level. The Gaussian 03 program package was used in the quantum chemical calculations (Frisch et al., 2003)). Thus, carnosine anions in the interlayer region form bilayers and GA anions monolayers, in which the carboxyl groups interact electrostatically with Al^{3+} of the upper and lower layers of the LDH matrix (Scheme 1). Hydrogen bonding between the layers and guest anions as well as interlayer water molecules also plays a role.

3.3. In vitro drug release behavior

Fig. 5 showed the accumulated amounts of drugs released into the buffer solution. A burst release phenomenon at the beginning of the tests was not observed. The carnosine-LDH in pH 7.4 PBS showed a gradual two-step release (Fig. 5a), with an early fast release (42.9% in the first 110 min) followed by a relatively slow one (71.1% in 750 min). GA-LDH showed a similar release pattern (Fig. 5b), with the released amount of 52.9% (in the first 210 min) during the rapid step and 61.1% (in 650 min) at equilibrium. The two-step and prolonged release behavior plays an important role in therapeutic treatments, as the initial fast release rapidly provides a therapeutic dose, and the subsequent sustained release maintains this dose over a long period of time. Another interesting observation was that the maximum release (in percent) of carnosine was larger than that of GA, which might be attributed to the stronger host-guest interactions between LDH and GA (by three hydroxyl groups in GA).

3.4. Mathematical modeling of drug release

To gain more insights into the mechanism of drug release, two types of kinetics models were exploited (Young et al., 2005; Kodama et al., 2001).

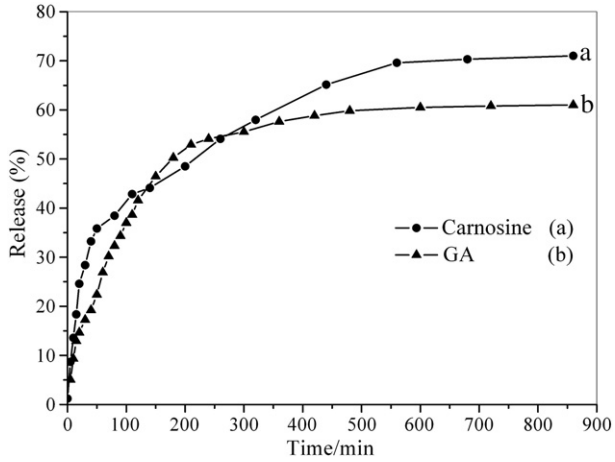

Fig. 5. *In vitro* release curves of (a) carnosine from carnosine-LDH and (b) GA from GA-LDH.

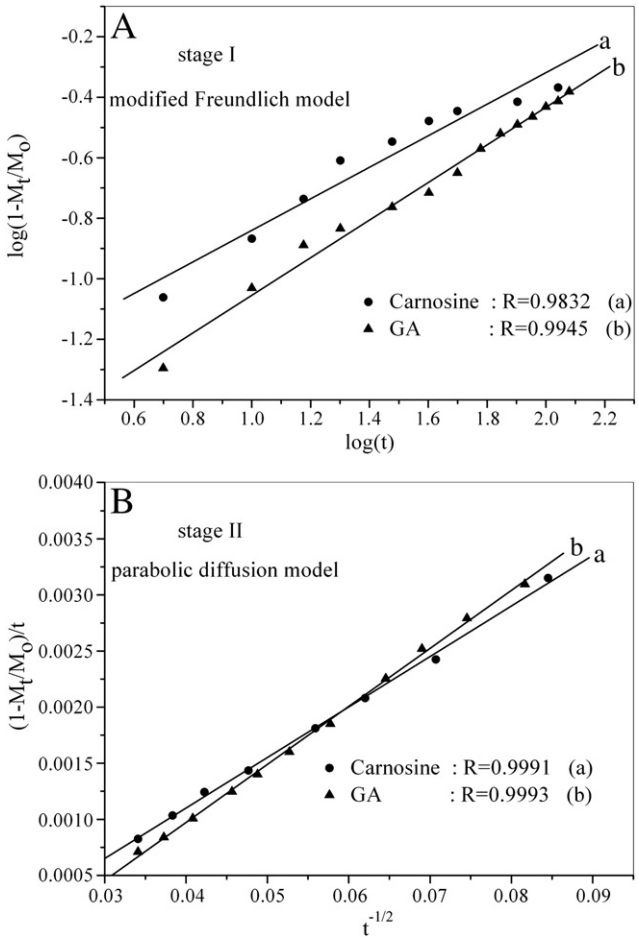

Fig. 6. Plots of the two kinetic models (A) modified Freundlich model and (B) parabolic diffusion model for the release of carnosine and GA from LDH in the two stages.

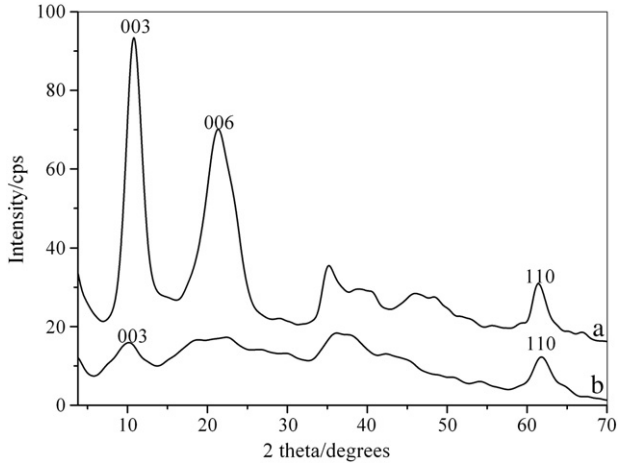

Fig. 7. XRD patterns of the solid residues of (a) carnosine-LDH-R and (b) GA-LDH-R.

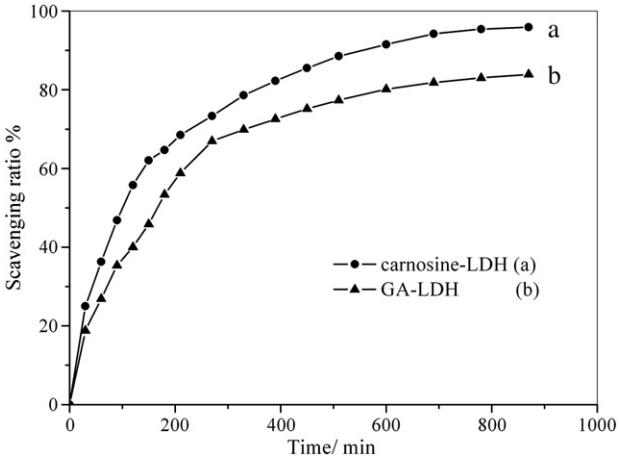

Fig. 9. Scavenging effect of (a) carnosine-LDH and (b) GA-LDH on DPPH (0.2 mg/ml) radical.

(1) The modified Freundlich model describes the release from a flat surface with heterogeneous sites based on a diffusion-controlled process:

$$(M_0 - M_t)/M_0 = kt^a \quad (1)$$

(2) The parabolic diffusion model elucidates that the release process is controlled by a diffusion process such as intraparticle diffusion or surface diffusion:

$$(1 - M_t/M_0)/t = kt^{-0.5} + b \quad (2)$$

where M_0 and M_t are the amounts of drug remained in the LDH at the release time 0 and t; k is the release rate constant, and a and b are constants whose chemical significance is not clearly resolved.

On the basis of the two kinetics models above, the fitting results of drug release profiles are given in Fig. S1. Both models did not fit the release data very well, with linear correlation coefficients of $R = 0.96 - 0.97$. This indicates that the whole drug release progress consists of more than one rate-determining step and thus cannot be described by a single kinetics model. To give a further insight of the release behavior, the whole progress was separated into two stages: the rapid release stage I followed by the slow release stage II. Fig. 6 displays the fitting, in which stage I and stage II were successfully simulated with the modified Freundlich model and parabolic diffusion model, with rather high linear correlation coefficients ($R = 0.98 - 0.99$). Based on the previous report that ion exchange cannot be the rate-determining step during the drug release process at pH = 7.4 (Zhang et al., 2006), the simulation results indicate that stages I and II can be described by external surface diffusion *via* ion exchange and the intraparticle diffusion.

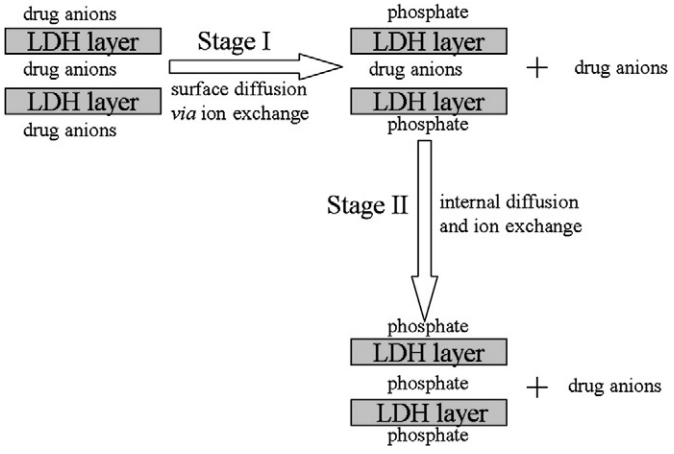

Fig. 8. Representation for drug release in buffer solution.

To better understand the release behavior, the solid residues of carnosine-LDH and GA-LDH after the release experiments were characterized by XRD (Fig. 7). Both d_{003} values (0.89 and 0.85 nm for carnosine-LDH-R and GA-LDH-R) were similar with the phosphate-LDH ($d_{003} = 0.88$ nm) (Costantino et al., 1997), indicating that the interlayer drug anions were phosphate anions of PBS. Furthermore, the FT-IR spectra of the drug-LDH-R displayed the characteristic band of phosphate centered at 1100 cm^{-1}, which is assigned to the δ(P—OH) and ν(P—O) stretching vibrations (Fig. S2). The mechanism proposed for release of carnosine and GA from the LDH matrix was displayed in Fig. 8. (1) The surface diffusion was the rate-controlling step in the release stage I. Drug anions on the external surface of LDH particles diffuse into the medium solution *via* anion exchange, accounting for the rapid drug release stage in Fig. 5. (2) Diffusion of drug anions from the interlayer space of LDH particles to the external surface became the rate-determining step in stage II, corresponding to the subsequent slow release period in Fig. 5. This two-step model prediction was consistent with the release progress of carnosine and GA.

3.5. Scavenging DPPH radicals

The scavenging ratio of DPPH increased with time (Fig. 9) until equilibrium was obtained (95.9% and 83.9% for carnosine-LDH and GA-LDH, normalized to the molar content of GA). The scavenging capacity of the antioxidant for DPPH was thus 10 g/mol (carnosine) and 8 g/mol (GA). In addition, two scavenging stages in whole progress were observed (a fast stage followed by a slow one), which was in accordance with the drug release behavior mentioned above. Therefore, LDH can be used as suitable drug delivery matrix for storing pharmaceutical agents, maintaining the bioactivity and achieving controlled release of antioxidant drugs.

4. Conclusions

This study demonstrated a facile approach for the incorporation of antioxidant drugs (carnosine and GA) into LDH. Carnosine-LDH and GA-LDH were obtained by ion exchange and coprecipitation. *In vitro* release studies showed a two-step release, without observing a burst phenomenon at the beginning of the release test. Two kinetics models were used to fit the release dynamics.

The release of drug anions can be described by external surface diffusion *via* ion exchange (stage I) and intraparticle diffusion (stage II). Carnosine and GA released from the LDH matrix served as excellent antioxidants to scavenge DPPH radicals (scavenging ratio: 95.9% for carnosine-LDH and 83.9% for GA-LDH in 870 min). Thus, MgAl/LDH can be used as an effective inorganic host matrix for the inhibition of the oxidation of antioxidant drugs during storage prior to application and for scavenging free radicals with controlled release properties.

Acknowledgments

This project was supported by the National Natural Science Foundation of China, the 111 Project (grant no. B07004), the 973 Program (grant no. 2009CB939802) and the Fundamental Research Funds for the Central Universities (grant no. ZZ0908).

Appendix A. Supplementary data

Supplementary data associated with this article can be found, in the online version, at doi:10.1016/j.clay.2010.06.017.

References

Ambrogi, V., Fardella, G., Grandolini, G., Perioli, L., 2001. Intercalation compounds of hydrotalcite-like anionic clays with antiinflammatory agents—I. intercalation and in vitro release of ibuprofen. Int. J. Pharm. 220, 23–32.

Azzam, T., Domb, A.J., 2004. Current development in gene transfection agents. Curr. Drug Deliv. 1, 165–193.

Barbe, C., Bartlett, J., Kong, L., Finnie, K., Lin, H.Q., Larkin, M., Calleja, S., Bush, A., Calleja, G., 2004. Silica particles: a novel drug-delivery system. Adv. Mater. 16, 1959–1966.

Bauer, L.A., Birenbaum, N.S., Meyer, G.J., 2004. Biological applications of high aspect ratio nanoparticles. J. Mater. Chem. 14, 517–526.

Bontchev, R.P., Liu, S., Krumhansl, J.L., Voigt, J., Nenoff, T.M., 2003. Synthesis, characterization, and ion exchange properties of hydrotalcite $Mg_6Al_2(OH)_{16}(A)_x(A')_{2-x}\cdot 4H_2O$ (A, A′ = Cl^-, Br^-, I^-, and NO_3^-, $2 \geq x \geq 0$) derivatives. Chem. Mater. 15, 3669–3675.

Choy, J.H., Kwak, S.Y., Park, J.S., Jeong, Y.J., 2001. Cellular uptake behavior of [γ-32P] labeled ATP-LDH nanohybrids. J. Mater. Chem. 11, 1671–1674.

Costantino, U., Casciola, M., Massinelli, L., Nocchetti, M., Vivani, R., 1997. Intercalation and grafting of hydrogen phosphates and phosphonates into synthetic hydrotalcites and a.c.-conductivity of the compounds thereby obtained. Solid State Ionics 97, 203–212.

Costantino, U., Ambrogi, V., Nocchetti, M., Perioli, L., 2008. Hydrotalcite-like compounds: versatile layered hosts of molecular anions with biological activity. Microporous Mesoporous Mater. 107, 149–160.

Couvreur, P., Dubernet, C., Puisieux, F., 1995. Controlled drug delivery with nanoparticles: current possibilities and future trends. Eur. J. Pharm. Biopharm. 41, 2–13.

Dagnon, K.L., Ambadapadi, S., Shaito, A., Ogbomo, S.M., Deleon, V., Golden, T.D., Rahimi, M., Nguyen, K., Braterman, P.S., D′Souza, N.A., 2009. Poly(L-lactic acid) nanocomposites with layered double hydroxides functionalized with Ibuprofen. J. Appl. Polym. Sci. 113, 1905–1915.

Decker, E.A., Livisay, S.A., Zhou, S., 2000. A reevaluation of the antioxidant activity of purified carnosine. Biochemistry 65, 766–770.

Dietz, G.P.H., Bahr, M., 2004. Delivery of bioactive molecules into the cell: the Trojan horse approach. Mol. Cell. Neurosci. 27, 85–131.

Feng, S.S., Chien, S., 2003. Chemotherapeutic engineering: application and further development of chemical engineering principles for chemotherapy of cancer and other diseases. Chem. Eng. Sci. 58, 4087–4114.

Fogg, A.M., Jenifer, S., Shyu, S.G., Cary, D.R., O'Hare, D., 1998. Selective ion-exchange intercalation of isomeric dicarboxylate anions into the layered double hydroxide $[LiAl_2(OH)_6]Cl\cdot H_2O$. Chem. Mater. 10, 351–355.

Fogg, A.M., Green, V.M., Harvey, H.G., O'Hare, D., 1999. New separation science using shape-selective ion exchange intercalation chemistry. Adv. Mater. 11, 1466–1469.

Friedman, M., Jürgens, H.S.J., 2000. Effect of pH on the stability of plant phenolic compounds. J. Agric. Food Chem. 48, 2101–2110.

Friedrich, J.O., Wasylishen, R.E., 1986. A proton and carbon-13 nuclear magnetic resonance study of carnosine. Can. J. Chem. 64, 2132–2138.

Frisch, M.J., Trucks, G.W., Schlegel, H.B., Scuseria, G.E., Rob, M.A., 2003. Gaussian 03, revision B.04. Gaussian Inc, Pittsburgh PA.

Galati, G., O'Brien, P.J., 2004. Potential toxicity of flavonoids and other dietary phenolics: significance for their chemopreventive and anticancer properties. Free Radic. Biol. Med. 37, 287–303.

Giannakopoulos, E., Christoforidis, K.C., Tsipis, A., Jerzykiewicz, M., Deligiannakis, Y., 2005. Influence of Pb( ) on the radical properties of humic substances and model compounds. J. Phys. Chem. A 109, 2223–2232.

Gomes, C.S.F., Silva, J.B.P., 2007. Minerals and clay minerals in medical geology. Appl. Clay Sci. 36, 4–21.

Hoyo, C.D., 2007. Layered double hydroxides and human health: an overview. Appl. Clay Sci. 36, 103–121.

José, G.L., Cristina, G.V., 2010. Vascular pro-oxidant effects secondary to the autoxidation of gallic acid in rat aorta. J. Nutr. Biochem. 21, 304–309.

Joshi, G.V., Patel, H.A., Kevadiya, B.D., Bajaj, H.C., 2009. Montmorillonite intercalated with vitamin B_1 as drug carrier. Appl. Clay Sci. 45, 248–253.

Kelner, A., Schacht, E.H., 2005. Tailor-made polymers for local drug delivery: release of macromolecular model drugs from biodegradable hydrogels based on poly (ethylene oxide). J. Control. Release 101, 13–20.

Khan, A.I., Lei, L., Norquist, A.J., O'Hare, D., 2001. Intercalation and controlled release of pharmaceutically active compounds from a layered double hydroxide. Chem. Commun. 2342–2343.

Kitts, D.D., Weiler, K., 2003. Bioactive proteins and peptides from food sources, applications of bioprocess used in isolation and recovery. Curr. Pharm. Des. 9, 1309–1323.

Kodama, T., Harada, Y., Ueda, M., Shimizu, K., Shuto, K., Komarneni, S., 2001. Selective exchange and fixation of strontium ions with ultrafine Na-4-mica. Langmuir 17, 4881–4886.

Kriven, W.M., Kwak, S.Y., Wallig, M.A., Choy, J.H., 2004. Bio-resorbable nanoceramics for gene and drug delivery. MRS Bull. 29, 33–37.

Kwak, S.Y., Kriven, W.M., Wallig, M.A., Choy, J.H., 2004. Inorganic delivery vector for intravenous injection. Biomaterials 25, 5995–6001.

Leroux, F., Maddar, L., Mailhot, B., Morlat-Therias, S., Gardette, J.L., 2005. Characterization and photooxidative behaviour of nanocomposites formed with polystyrene and LDHs organo-modified by monomer surfactant. Polymer 46, 3571–3578.

Leroux, F., Illaik, A., Verney, V., 2009. A comprehensive study of an unusual jammed nanocomposite structure using hybrid layered double hydroxide filler. J. Colloid Interface Sci. 332, 327–335.

Minko, T., 2004. Drug targeting to the colon with lectins and neoglycoconjugates. Adv. Drug Deliv. Rev. 56, 491–509.

Prevot, V., Forano, C., Besse, J.P., 1998. Syntheses and thermal and chemical behaviors of tartrate and succinate intercalated Zn_3Al and Zn_2Cr layered double hydroxides. Inorg. Chem. 37, 4293–4301.

Shi, W.Y., Wei, M., Jin, L., Li, C.J., 2007. Calcined layered double hydroxides as a "biomolecular vessel" for bromelain: immobilization, storage and release. J. Mol. Catal. B Enzym. 47, 58–65.

Tammaro, L., Costantino, U., Nocchetti, M., Vittoria, V., 2009. Incorporation of active nano-hybrids into poly(ε-caprolactone) for local controlled release: antifibrinolytic drug. Appl. Clay Sci. 43, 350–356.

Terashima, M., Nakatani, I., Harima, A., Nakamura, S., Shiiba, M., 2007. New method to evaluate water-soluble antioxidant activity based on protein structural change. J. Agric. Food Chem. 55, 165–169.

Theodorou, D.N., 2007. Hierarchical modelling of polymeric materials. Chem. Eng. Sci. 62, 5697–5714.

Tyner, K.M., Roberson, M.S., Berghorn, K.A., Li, L., Gilmour, R.F., Batt, C.A., Giannelis, E.P., 2004. Intercalation, delivery, and expression of the gene encoding green fluorescence protein utilizing nanobiohybrids. J. Control. Release 100, 399–409.

Vaughan-Jones, R.D., Spitzer, K.W., Swietach, P., 2006. Spatial aspects of intracellular pH regulation in heart muscle. Prog. Biophys. Mol. Biol. 90, 207–224.

Wei, M., Zhang, X., Evans, D.G., Duan, X., Li, X.J., Chen, H., 2007. Rh-TPPTS intercalated layered double hydroxides as hydroformylation catalyst. American Institute of Chemical Engineers Journal 53, 2916–2924.

Wei, M., Pu, M., Guo, J., Han, J.B., Li, F., He, J., Evans, D.G., Duan, X., 2008. Intercalation of L-dopa into layered double hydroxides: enhancement of both chemical and stereochemical stabilities of a drug through host–guest interactions. Chem. Mater. 20, 5169–5180.

Williams, G.R., O'Hare, D., 2006. Towards understanding control and application of layered double hydroxide chemistry. J. Mater. Chem. 16, 3065–3074.

Xu, Z.P., Zeng, Q.H., Lu, G.Q., Yu, A.B., 2006. Inorganic nanoparticles as carriers for efficient cellular delivery. Chem. Eng. Sci. 61, 1027–1040.

Young, C.R., Dietzsch, C., Cerea, M., Farrell, T., Fegely, K.A., Rajabi-Siahboomi, A., McGinity, J.W., 2005. Physicochemical characterization and mechanisms of release of theophylline from melt-extruded dosage forms based on a methacrylic acid copolymer. Int. J. Pharm. 301, 112–120.

Yu, J.J., Cheng, J., Ma, C.Y., Wang, H.L., Li, L.D., Hao, Z.P., Xu, Z.P., 2009. NO_x decomposition, storage and reduction over novel mixed oxide catalysts derived from hydrotalcite-like compounds. J. Colloid Interface Sci. 333, 423–430.

Zhang, H., Zou, K., Guo, S.H., Duan, X., 2006. Nanostructural drug-inorganic clay composites: structure, thermal property and in vitro release of captopril-intercalated Mg–Al-layered double hydroxides. J. Solid State Chem. 179, 1792–1801.